Steel and Composite Structures, *Vol. 34, No. 4 (2020) 525-545*
DOI: https://doi.org/10.12989/scs.2020.34.4.525

Flexural performance of composite walls under out-of-plane loads

Saeid Sabouri-Ghomi[1a], Arman Nasri[1b], Younes Jahani[2c] and Anjan K. Bhowmick[*3]

[1]*Civil Engineering Department, K.N. Toosi University of Technology, Tehran, Iran*
[2]*Analysis and Advanced Materials for Structural Design (AMADE), Polytechnic School, University of Girona, Girona, Spain*
[3]*Department of Building, Civil and Environmental Engineering, Concordia University, Montreal, Canada*

(*Received August 13, 2019, Revised December 26, 2019, Accepted January 3, 2020*)

Abstract. This paper presents a new structural system to use as retaining walls. In civil works, there is a general trend to use traditional reinforced concrete (RC) retaining walls to resist soil pressure. Despite their good resistance, RC retaining walls have some disadvantages such as need for huge temporary formworks, high dense reinforcing, low construction speed, etc. In the present work, a composite wall with only one steel plate (steel–concrete) is proposed to address the disadvantages of the RC walls. In the proposed system, steel plate is utilized not only as tensile reinforcement but also as a permanent formwork for the concrete. In order to evaluate the efficiency of the proposed SC composite system, an experimental program that includes nine SC composite wall specimens is developed. In this experimental study, the effects of different parameters such as distance between shear connectors, length of shear connectors, concrete ultimate strength, use of compressive steel plate and compressive steel reinforcement are investigated. In addition, a 3D finite element (FE) model for SC composite walls is proposed using the finite element program ABAQUS and load-displacement curves from FE analyses were compared against results obtained from physical testing. In all cases, the proposed FE model is reasonably accurate to predict the behavior of SC composite walls under out-of-plane loads. Results from experimental work and numerical study show that the SC composite wall system has high strength and ductile behavior under flexural loads. Furthermore, the design equations based on ACI code for calculating out-of-plate flexural and shear strength of SC composite walls are presented and compared to experimental database.

Keywords: composite wall system; retaining wall; experimental work; FE model; flexural load

1. Introduction

Nowadays, in construction projects, such as in roads, bridges, and building constructions, retaining walls are used to resist lateral soil pressure. These walls are also used to withstand the water pressure in coastal structures and ice-moving pressure in marine structures. In high-rise buildings, due to different reasons such as to reach to the proper and strong bedrock for foundation, to provide adequate parking space for the vehicles, to increase the architectural space, deep excavations are planned. During the construction of tall buildings, to deal with the soil pressure in deep excavation, simple methods such as nailing are utilized. However, with time due to earthquakes or landslides, the nailing may lose its resistance. Therefore, retaining walls would be an effective method to resist out-of-plane loads.

*Corresponding author, Ph.D.
E-mail: anjan.bhowmick@concordia.ca
[a]Professor
E-mail: sabouri@kntu.ac.ir
[b]Ph.D. Student
E-mail: anasri@mail.kntu.ac.ir
[c]Ph.D. Student
E-mail: younes.jahani@yahoo.com

In general, reinforced concrete (RC) system is utilized to construct the retaining walls. High ductility and high strength are some of the advantages of RC system. On the other hand, need for huge temporary formworks, high dense reinforcing, low construction speed, engaging a large number of workers, etc. are some of the disadvantages of this system (Yan *et al.* 2018, Sener *et al*. 2015, Qin *et al.* 2019). The low construction speed of RC retaining walls has effects on the total construction time of the project. Due to these disadvantages, the idea of using composite (steel–concrete) SC walls as retaining walls comes into authors' mind. This SC composite system contains one steel plate, concrete cover, shear connectors and reinforcement network. The steel plate is placed on the interior side of the wall and concrete and reinforcements are placed on the exterior side of the wall and near to the soil. The concrete is attached to the plate using the shear connectors. The steel plate in SC composite walls can be replaced with the steel reinforcement bars in RC walls and it can also be used as an exterior permanent formwork for the concrete. Thus, use of SC composite walls, instead of RC walls, can significantly increase the speed of construction. Fig. 1 shows the details of the proposed SC composite wall.

In order to construct these SC composite walls, first, steel plate with shear connectors is welded to the surrounding frame (beams and columns) within the story, then reinforcements are placed in the appropriate position and finally, concrete is cast. However, due to low flexural strength of the steel plate, during the concrete casting, some

http://www.techno-press.org/?journal=scs&subpage=6
ISSN: 1229-9367 (Print), 1598-6233 (Online)

temporary supports should be used behind the steel plate until the concrete reaches to sufficient strength. In real projects, the length of retaining wall is larger than its height; therefore, the wall behaves similar to one-way slab and the soil pressure will be transferred to the structure through the upper and lower beams.

Shear connectors are used to attach the concrete to the steel plate. By increasing the number of the shear connectors, the slip between the concrete and steel plate can be decreased and the behavior of the wall will be near to the full composite action. The shear connectors are fabricated in different shapes such as angles, channels, hooks and studs. They are not only used to decrease the slip between the layers but can also be used as a shear reinforcement (stirrups) to resist the shear force.

In the past two decades, due to importance of composite structures, different studies have been carried on the composite systems. Solomon *et al*. (1976) studied the behavior of composite beams and walls. They conducted experimental works to determine the failure modes of the specimens. Oduyemi and Wright (1989) studied the effects of different parameters on the behavior of composite beams. Wright et al. (1991) presented an analytical method to analyze and design of composite structure. Furthermore, the effect of hooked-shape shear connectors on the behavior of composite beams and slabs have been studied by Liew and Sohel (2009) and Sohel and Liew (2011).

Dogan and Roberts (2010) compared the results of experimental works of composite beams with the results of partial and full interaction theory. Xie *et al*. (2007) investigated the behavior of composite beams with experimental and analytical works. They found that most proper and ductile behavior of composite beams happened by yielding the steel plate prior to failure.

Many researchers (Sener *et al.* 2016, Sener and Varma 2014) studied the behavior of composite beams under out-of-plane loads. They compared the results of experimental tests with different design codes. Turmo *et al*. (2015) presented FE method to analyze the composite beams with partial interaction theory. Yun *et al.* (2014, 2015) conducted different analytical and experimental works on the behavior of composite beams and shear connectors. Partial interaction theory was used by many researchers to analyze composite beams (Ranzi *et al.* 2003, Ranzi 2006, Cas *et al*. 2004). Fanaie *et al*. (2015) conducted an analytical study on composite beams with different arrangements of channel shear connectors. Ding *et al*. (2016) studied the flexural stiffness of steel-concrete composite beam under a positive moment.

Numerous studies have been carried out to investigate the behavior of composite walls under in-plane loadings. Kurt *et al.* (2016) studied the behavior of composite walls without boundary elements under in-plane loads. They presented some equations to predict the capacity of composite walls. Seo *et al.* (2016) used several experimental tests to evaluate the accuracy of the design codes to calculate the shear capacity of composite walls. Hossain and Wright (2004) presented an analytical formulation to calculate the strength and stiffness of the composite walls. They used experimental tests to validate their proposed formulations. Zhao and Astaneh-Asl (2004) performed cyclic loading tests on composite walls. They concluded that small gap between concrete cover and the surrounding frame can increase the ductility of composite walls. In a similar study, Zhao *et al.* (2016) studied the hysteric model of composite walls. Ji et al. (2017) studied the behavior of composite walls with high ratio of steel. These kinds of walls are typical systems in high-rise buildings. Epackachi *et al.* (2014) conducted experimental work and numerical simulation to investigate the resistance of composite walls under lateral loading.

Furthermore, the behavior of composite walls under compressive load has been investigated in different analytical, numerical and experimental studies. Yung *et al*. (2016) used ten experimental specimens to study the effect of shear connectors pattern and width to thickness ratio on the behavior of composite walls. They presented an equation based on Euler equations to predict the buckling stresses. Huang and Liew (2016) studied the behavior of composite walls with hooked-shape shear connectors. Their study showed that hooked-shape shear connectors increased the efficiency of composite walls. Prabha *et al*. (2013) studied the effect of confinement on the compressive behavior of composite walls. It was observed that by increasing the confinement (provided by shear connectors), the compressive strength of composite wall was increased.

The present study is a part of ongoing comprehensive research at the K. N. Toosi University of Technology. First, Sabouri *et al.* (2016) presented a new closed form solution based on the Partial-Interaction Theory to analyze the SC composite walls under out-of-plane loads.

In the present work, to address the disadvantages of the concrete reinforcement walls, SC composite system is presented to use as retaining walls. This study is classified into three phases: experimental works, numerical works and analytical work.

In the first phase of the study, nine specimens are tested under out-of-plane loads. In this phase, effect of different parameters on the behavior of SC composite walls is studied. Furthermore, a comparison is conducted between the results of RC and SC walls. Unlike previous works, where sandwich systems (steel–concrete–steel) were used, in the proposed system, only one steel plate is used (steel–concrete).

In the second phase of this study, numerical analysis is performed using ABAQUS software. Each experimental specimen is simulated in ABAQUS software and compared with test results. The objective of the second phase of this study is to develop a reliable numerical tool which can be used to conduct parametric study in the future. In the third phase, flexural and shear strength of the proposed SC composite system are obtained according to the design methodology in ACI 318-05 code.

2. Experimental program

2.1 Test setup

An experimental program that included nine specimens was designed to investigate the behavior of SC composite

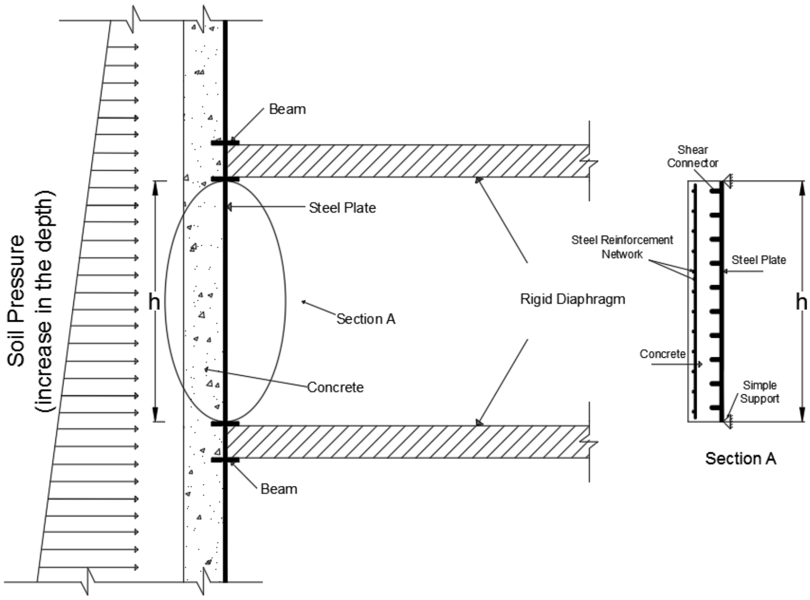

Fig. 1 Details of SC composite wall

Fig. 2 (a) Shear connectors welded to steel plate and (b) Bending test on the shear stud

walls under out-of-plane loads. The effect of different parameters was investigated in the experimental study. Nine specimens were named as W1 to W9. The length and height of the retaining walls were equal to 4 m and 3 m, respectively. Due to limitations in the laboratory, W1 to W3 specimens were built on one-third scale. Therefore, the length and height of these specimens were 1.3 m and 1 m, respectively. After testing the first three walls, it was observed that the behavior of the retaining walls was similar to one-way slabs under out-of-plane loads. Thus, the length of the rest of the specimens (i.e., W4 to W9) was reduced to 0.35 m to cover the laboratory limitations and save in the fabrication costs. All specimens were built by SC composite system except the W3 specimen, which was fabricated with RC system to compare with SC composite walls. In all specimens of SC composite walls, the thickness of steel plate and concrete cover were equal to 2 mm and 100 mm, respectively. In addition, shear connectors of 10 mm diameter were used to connect the steel plate and concrete cover. Fig. 2(a) shows the welded shear connectors in the W1 specimen. An arc-welding process was used to weld the shear connectors to the steel plate. According to American Welding Society standard (AWS 2010), a steel pipe was utilized to bend the shear connectors. The suggested angle is 30 degrees (Fig. 2(b)). To avoid melting the thin steel plate during the welding, an expert welder was employed.

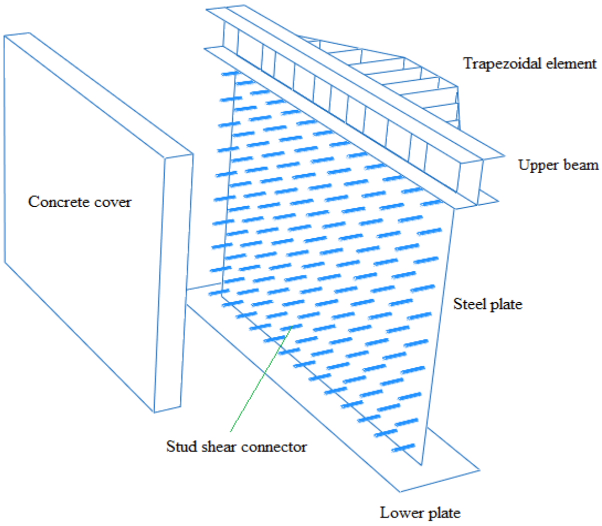

Fig. 3 Details of SC composite walls with boundary elements (upper beam and lower plate)

Table 1 Details of SC composite walls

Specimens	W1	W2	W4	W5	W6	W7	W8	W9
Length (mm)	1300	1300	350	350	350	350	350	350
Height (mm)	1000							
Plate thickness (mm)	2							
Concrete thickness (mm)	100							
Shear connector spacing (mm)	100	200	100	100	100	100	350	100
Shear connector length (mm)	85	85	85	40	40	85	85	85
Concrete cubic strength (Mpa)	28.4	28.4	28.4	28.4	28.4	45.2	28.4	28.4
With compressive plate	×	×	×	×	✓	×	×	×
With compressive reinforcement	×	×	×	×	×	×	×	✓

The connections between the specimen and the supports were provided by lower plate and upper beam. The lower plate was used to connect the lower part of the specimen to the rigid floor and the upper beam was used to connect the upper part of the specimen to the rigid frame. Furthermore, the upper beam was connected to the rigid frame through the trapezoidal element. Therefore, the boundary conditions of the specimens were similar to those in the retaining walls in real life projects. Due to the large length of the retaining walls, the columns have minor effects on the flexural stiffness of the wall; therefore, the columns were not fabricated in the experimental specimens. Fig. 3 shows the configuration of the W1 specimen.

In the W2 specimen, the spacing between the shear connectors was doubled in comparison to the W1 specimen. In other words, the spacing between shear connectors in both directions were 100 mm and 200 mm in W1 and W2 specimens, respectively.

As previously mentioned, the length of the rest of the SC specimens was reduced to 0.35 m. Therefore, the only difference between the W4 and the W1 specimen was the length of the wall. W4 specimen was considered as a reference of SC composite wall to compare with other specimens (i.e. W5 to W9). In W5 to W9 specimens, only one parameter was changed in comparison to W4 specimen to study the effect of different parameters on the behavior of SC composite walls. To evaluate the effect of the shear connector length, W5 specimen was fabricated with 40 mm shear connector length. In the W4 specimen, the shear connector length was 85 mm. The effect of steel plate in the compressive side (steel–concrete–steel) was assessed in the W6 specimen. In the W7 specimen, the influence of high concrete compressive strength was investigated on the behavior of SC composite wall. A concrete with strength of 45.2 MPa was used in this specimen.

As mentioned previously, the effect of shear connector spacing was considered in the W1 and W2 specimen, but to investigate the effect of the large and unusual distance between the shear connectors on the failure mode of the SC wall, W8 specimen was tested in the laboratory. The distance between the shear connectors was 350 mm and 100 mm for W8 and W4 specimens, respectively. In W9 specimen, a reinforcement network was utilized in the compressive side of the wall to evaluate the effect of existence reinforcement in the compressive side of the section on the behavior of SC composite wall. Table 1 shows the details of the SC composite walls.

Table 2 Details of W3 specimen

W3 Specimen	
Length (mm)	1300
Height (mm)	1000
Thickness (mm)	140
Vertical tensile reinforcement (mm)	10 T 14 @ 133
Vertical compressive reinforcement (mm)	10 T 8 @ 133
Horizontal reinforcement in both sides (mm)	5 T 8 @ 200

In order to compare the results of SC and RC walls under out-of-plane loading, W3 specimen was built as a reinforced concrete wall. It was designed to have same resistance as W1 specimen. The thickness of concrete was 140 mm with covers for tensile and compressive steel reinforcements. The diameter of the vertical bars in the tensile and compressive side was 14 mm and 8 mm, respectively. In addition, the distance between these bars on both sides was 133 mm. Furthermore, five bars with diameter of 8mm and space of 200 mm were used as horizontal reinforcements on both sides. These reinforcement networks were hold by link bars. To connect the wall to the lower plate and upper beam, a steel plate with 100 mm width and 3 mm thickness was utilized. Table 2 shows the details of the W3 specimen.

In general, four different failure modes can be considered in composite walls under out-of-plane loads: flexural failure mode, transverse shear failure mode, interfacial shear failure mode and bucking failure mode. The most appropriate failure mode of composite wall is the flexural failure mode, which can provide high ductility before failure. To avoid interfacial shear failure i.e. slip between the layers, the space between the shear connectors should satisfy the following equation (Zhang *et al.* 2013)

$$S < \sqrt{\frac{Q_n h}{2F_{yp}\ t_p}} \tag{1}$$

where h is the height of the wall, F_{yp} is the yield stress of the steel plate, t_p is the thickness of the steel plate, Q_n is the shear capacity of single shear connector and can be derived by Eq. (2) according to Eurocode 4 (2009).

$$Q_n = \min\left\{\begin{matrix} Q1 = 0.8F_{us}\left(\frac{\pi}{4}d_s^2\right)/\eta \\ Q2 = 0.29\alpha\, d_s^2\sqrt{f_c' E_c}/\eta \end{matrix}\right\} \tag{2}$$

where d_s is the diameter of the shear connector, F_{us} is the ultimate strength of the shear connector, f_c' is the ultimate strength of concrete, E_c is the modulus elasticity of concrete, η is the reduction factor (considered equal to 1.0); α is a factor calculated according to Eq. (3)

$$\left\{\begin{matrix} \alpha = 0.2\left(\frac{h_s}{d_s}+1\right) & for \quad 3 < \frac{h_s}{d_s} < 4 \\ \alpha = 1 & for \quad \frac{h_s}{d_s} > 4 \end{matrix}\right\} \tag{3}$$

where h_s is the height of the shear connector.

Using Eq. (1), the allowable spacing between the shear connectors was calculated as 140 mm in all SC composite walls. Therefore, it was expected that W2 and W8 specimens would fail in the interfacial shear mode.

2.2 Test limitations

The main limitations of this study were related to specimen dimensions, loading procedure and capacity of hydraulic jack. In the retaining walls, the loading along the wall's height should be linearly (triangular) distributed i.e. the amount of load at the top of the wall is zero and at the bottom of the wall is maximum. To apply the distributed load, airbags can be utilized. However, in the airbag loading procedure, the load will be distributed uniformly on the wall surface, which does not simulate the triangular loading condition. Therefore, in this study, it was decided to apply the equilibrium load. Theoretically, the equilibrium resultant load should be applied at one third of the wall's height, but due to the following reasons the load was applied in the middle of the wall:

- The main aim of this research was to investigate the flexural behavior of the composite walls under out-of-plane loads and therefore, the type as well as exact location of the loading was not the main parameters.
- Applying the load at one third of the wall's height was not possible in the laboratory.
- In deep excavations (tall buildings), the soil pressure is applied to retaining wall as a trapezoidal load (Fig. 1). Therefore, the location of the resultant load will be moved from one third towards the middle of the wall's height.
- In the retaining walls, during an earthquake, the location of the resultant load will be moved towards the middle of the wall.
- The retaining walls and the marine structures may be subjected to different types of loads. For instance, in the marine structures, the walls will be subjected to concentrated loads (due to ice-moving) and it can be applied to any part of the wall.

(a) (b)

Fig. 4 (a) Test set-up details and (b) loading beam

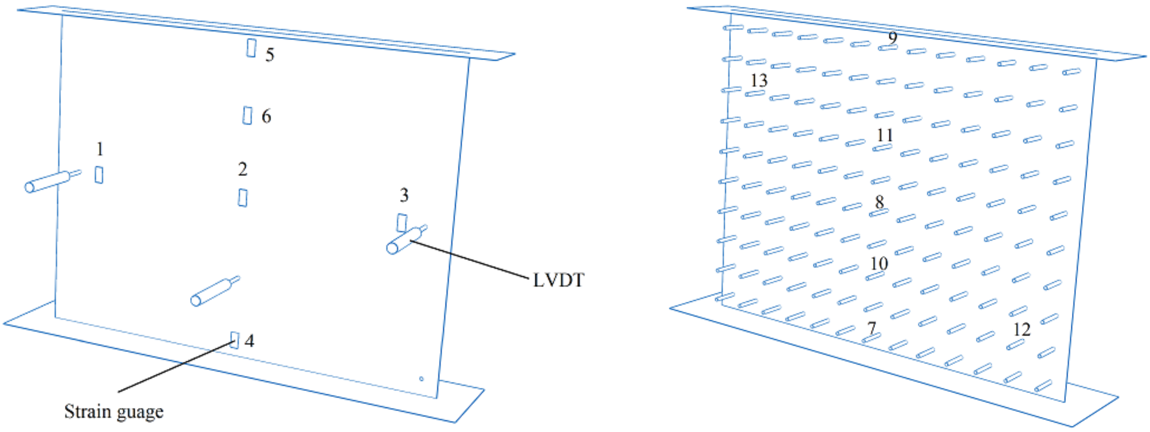

(a) (b)

Fig. 5 Arrangement of LVDTs and strain gauges on SC composite wall: (a) three LVDTs and six strain gauges on steel plate and (b) seven strain gauges on shear connectors

For load application, static push loading was applied in the middle of the specimens using a rigid beam in the form of displacement control. A 50-ton hydraulic actuator with a 300 mm stroke was used to apply the load. Furthermore, for smooth and uniform distribution of the loads, a thin elastomeric layer was used between the rigid beam and the specimens (Fig. 4 (b)).

In order to record the displacement and strain of the specimens, three linear variable displacement transducers (LVDTs) and 13 linear strain gauges were utilized. The LVDTs were installed on the tensile surface of the wall in three locations and the strain gauges were installed on the steel plate and the shear connector's shank. Fig. 5 shows the locations of LVDTs and strain gauges for W1 specimen.

2.3 The mechanical properties of material

An experimental program was carried out to characterize the material properties and obtain the mechanical properties of the materials involved in the specimens. Table 3 shows the results of material tests. Three cubes were considered to determine the compressive strength of the concrete. Furthermore, to characterize the mechanical behavior of the steel materials, three specimens were tested for the steel plate and the shear connectors. The mean value, standard deviation and coefficient of variation are summarized in Table 3.

3. Test observations

In this section, test observation for each specimen is presented. The results for W1 to W9 specimens are shown in Table 4. Furthermore, the load-displacement curves for the specimens are shown in Fig. 6.

3.1 W1 specimen

Fig. 7 shows the deformed shape of W1 specimen at the end of the test. This wall showed a flexural behavior with yielding in the steel plate and excessive tensile concrete cracks in the mid-height of the specimen.

Table 3 Material test results

Material test program	Mean value	Standard deviation	Coefficient of variation (%)
Cubic compressive Strength of normal strength concrete (MPa)	27.9	0.49	1.76
Modulus of elasticity of normal strength concrete (GPa)	22.2	0.16	0.74
Cubic compressive Strength of high strength concrete (MPa)	45.17	1.27	2.8
Modulus of elasticity of high strength concrete (GPa)	31.53	0.41	1.3
Yield strength of steel plate (MPa)	249.83	0.45	0.18
Ultimate strength of steel plate (MPa)	305.43	1.53	0.5
Yield strength of shear connector (MPa)	300.5	2.37	0.78
Ultimate strength of shear connector (MPa)	330.47	4.29	1.3

Table 4 Result of experimental tests

Specimens	Yield displacement (m m)	Yield force (KN)	Elastic stiffness (KN/m)	Ultimate displacement (mm)	Ultimate for ce (KN)	Ductility index Rati o	Failure mode*
W1	5.5	330	56	50	442	9.1	F
W2	8.5	280	40	50	350	5.9	F
W3	7.2	324	44	38	471	5.3	F
W4	6.1	71	11.2	50	102	8.2	F
W5	5.9	73	11.8	17.2	86.6	2.9	F-S
W6	6.6	87	11.4	22.4	122	3.4	F-S
W7	6.7	73	10.8	50	106	7.5	F
W8	9.7	76	8.9	37.5	87	3.9	F-W
W9	6.7	84	11.2	46	109	6.9	F

*Failure modes: (F: flexural failure; F-S: flexural failure followed by shear failure; W: welding fracture)

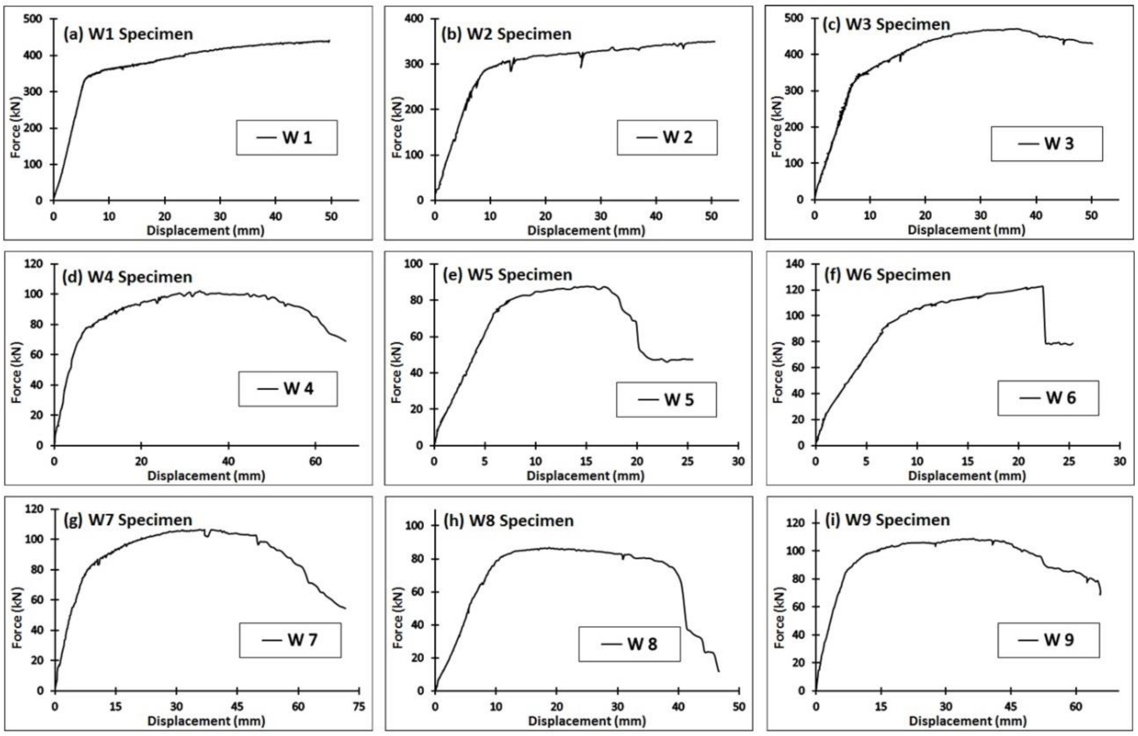

Fig. 6 Experimental load-displacement curves of specimens

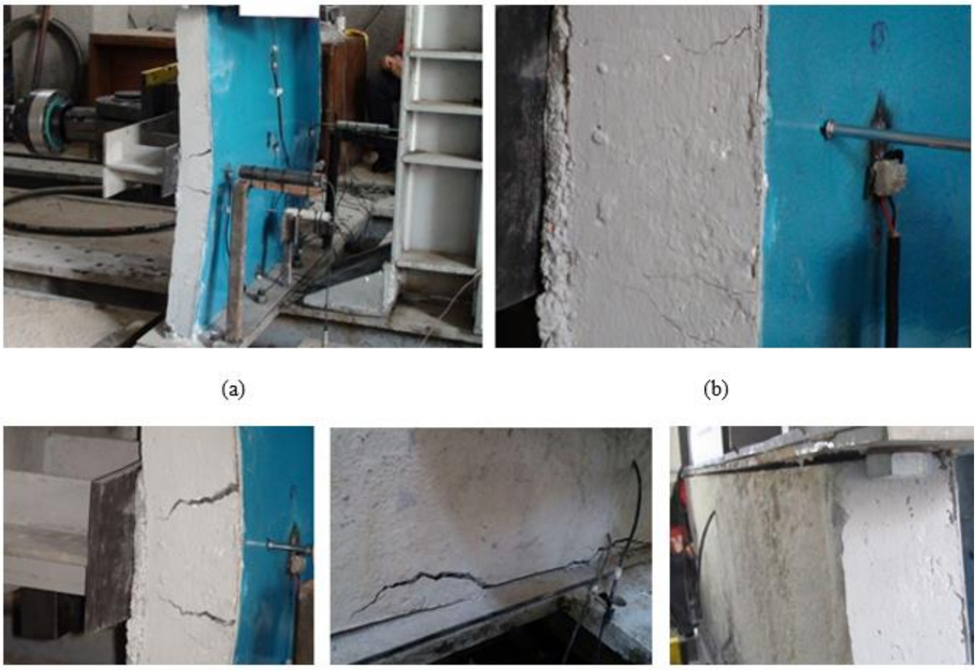

(a) (b)

(c) (d) (e)

Fig. 7 W1 specimen: (a) Deformed shape of the wall, (b) Crack width at the beginning of the test, (c) Crack width at the end of the test, (d) Concrete splitting and (e) Concrete rotating

The load-displacement curve for the W1 specimen is shown in Fig. 6(a). The yield strength, ultimate strength, elastic stiffness and yield displacement of this specimen were 330 kN, 442 kN, 56 kN/m and 5.5 mm, respectively. The specimen failed in flexural mode with high ductility. Due to smaller spacing between the shear connectors, i.e., less than the allowable value calculated from Eq. (1), no slip failure has been observed in the W1 specimen.

During the test, due to limitations in the hydraulic jack stroke, it was not possible to record the descending branch of the curve. However, the deflection in the middle of specimen was recorded up to 50 mm. The ductility index (i.e. ratio of ultimate displacement to yield displacement) was about 9.1, which indicated high ductility of this specimen. At the beginning of the test, the specimen was completely in the elastic state and no damage was observed. By increasing the load, flexural micro cracks appeared on the tensile side of the concrete. The width of the cracks was increased from 0.5 mm at the beginning of the test to 10 mm at the end of test. The upper and lower parts of the concrete started to rotate and separated from supports due to large deformations of specimen.

According to ACI 318-05 (2005), to avoid the shear failure in RC beams, the maximum spacing between the shear reinforcement is limited to half of the effective depth of the cross section (d/2). As mentioned previously, in the SC composite walls, the shear connectors not only attach the steel plate to the concrete, but also act as stirrups against transverse shear loads. Therefore, short distance between the shear connectors can prevent the transverse shear failure in the specimen. In the case of transverse shear failure, the force-displacement curve falls suddenly with low ductility and the tensile diagonal cracks appear with a 45-degree angle in the wall section. In W1 specimen, the distance between the shear connectors was 100 mm (i.e. twice the limitation of ACI for RC elements). Despite the larger spacing between the shear connectors, neither collapse in the load-displacement curve nor tensile diagonal cracks in the wall section were observed.

The strain data for strain gauges No. 1, 5, and 10 was plotted in Fig. 8. The ratio of strain to yield strain for the gauge No. 1 (in the middle of the specimen) was 15. Therefore, the middle part of the steel plate was completely yielded. In addition, strain gauges No. 5 and 10 (placed at the top of the plate and on the shear connector shank, respectively), were remained in their elastic phases. Since the strain gauge No. 1 failed at a strain equivalent to 15 ε_y, it was not possible to record the strain until the end of the test.

3.2 W2 Specimen

In the W2 specimen, the distance between the shear connectors was increased to 200 mm to evaluate the effect of shear connector's spacing on the performance of the SC composite wall under out-of-plane loads. Fig. 9 shows the deformed shape of the W2 specimen at the end of the test. Due to large spacing between the shear connectors (twice in compare to W1), it was expected to fail in interfacial shear, but similar to W1 specimen, it experienced a flexural behavior with yielding of the steel plate and concrete cracking in the tensile region. According to Eq. (1), the allowable distance between the shear connectors to prevent

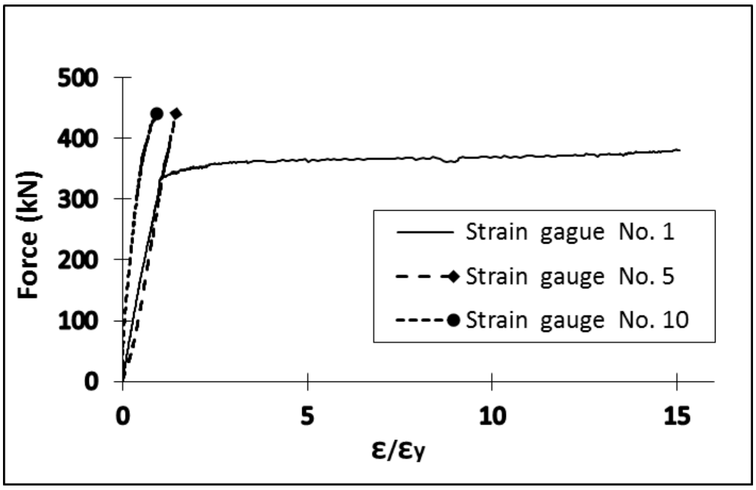

Fig. 8 Force - strain curves for three linear strain gauges

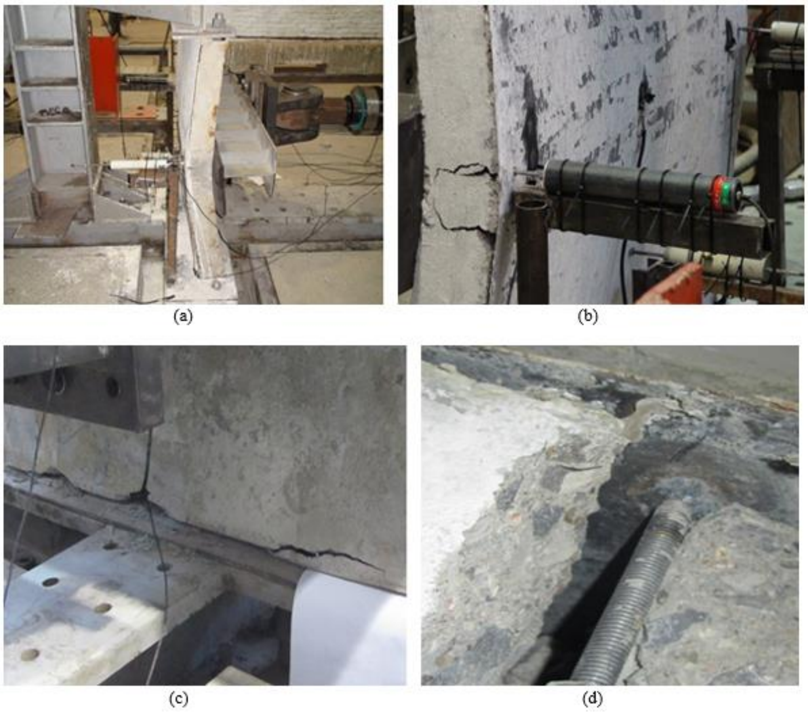

Fig. 9 W2 specimen: (a) Deformed shape of the wall, (b) Excessive crack in concrete, (c) Concrete splitting (d) No shear failure in shear connector

of interfacial shear failure mode was 140 mm. It was found that even at a distance of 200 mm, no slip failure was occurred and the wall showed a flexural behavior with a high degree of ductility. The reason for this behavior was due to the welding line between the steel plate and boundary elements. This welding line endured a large amount of the interfacial shear force developed between the steel plate and concrete and therefore, only small amount of shear force was shared between shear connectors. As shown in Fig. 6(b), the yield strength, ultimate strength, elastic stiffness, and yield displacement for W2 specimen were 280 kN, 350 kN, 40 kN/mm and 8.5 mm, respectively. Similar to W1 specimen, due to limitations of the hydraulic jack stroke in the laboratory, it was not possible to record the descending branch of the load-displacement curve. However, the deflection in the middle of the specimen was recorded up to 50 mm. The ductility index was calculated as 5.9.

At the beginning of the test, the W2 specimen was in the elastic phase. At a displacement of 2 mm and at a force of 117 kN, the first tensile crack was appeared in the concrete in the maximum moment region. The second crack was appeared at a displacement and force of 3.5 mm and 145 KN, respectively. To see the yielding process in the steel

Fig. 10 Deformed shape of W3 specimen

Fig. 11 Deformed shape of W4 specimen

plate, the back surface of the steel plate was covered with limewater. At a displacement of 6 mm and a force of 250 kN, the surface of the concrete started to split. The concrete splitting was increased at the end of the test (Fig. 9). In addition, similar to W1 specimen, at a force of 250 kN, the upper and lower parts of the concrete started to rotate and separated from the surrounding elements.

Despite the large spacing between the stirrups in this specimen, (i.e., four times the limitation of ACI), neither sudden fracture in the load-displacement curve nor diagonal cracks in the wall section were seen in the W2 specimen. Therefore, unlike RC walls, the spacing between shear studs (stirrups) can be considered equal to “2d” in the SC composite walls. This was found to be an important advantage of SC composite walls in comparison to RC walls.

3.3 W3 specimen

To compare the behavior of the SC composite walls with the RC walls under out-of-plane loads, the W3 specimen was built with RC system. The deformed shape of this specimen at the end of the test is shown in Fig. 10. Different flexural cracks were observed at the center of the wall. According to the load-displacement curve in Fig. 6(c), the yield strength, ultimate strength, elastic stiffness, and yield displacement of the W3 specimen were 324 kN, 471 kN, 44 kN/mm and 7.2 mm, respectively. At a displacement of 1.5 mm and a force of 95 kN, the first flexural crack was observed in the specimen. The number of these cracks tripled at a deflection equal to 2.9 mm and a force of 168 kN. With increase in the load, the depth and width of these cracks increased significantly. Finally, the specimen failed at a deflection of 38 mm. The ductility index for this specimen was equal to 5.3.

3.4 W4 specimen

W4 specimen was the reference specimen to compare with W5 to W9 specimens. This wall was similar to W1 specimen and only the length of the wall was reduced to 0.35 m. Ductile behavior was observed at the end of the test and the specimen failed by yielding in the steel plate and cracking in the concrete. Fig. 11 shows the deformed shape of this specimen. At a force equal to 9.0 kN and at a displacement equal to 0.2 mm, the first crack was observed in the specimen. With the increase in the load, the number, width and depth of the cracks were increased. The load-

Fig. 12 Deformed shape of W5 specimen

Fig. 13 Deformed shape of W6 specimen

displacement curve for the W4 specimen is shown in Fig. 6(d). For this specimen, the yield strength, ultimate strength, elastic stiffness, and yield displacement were 71 kN, 102 kN, 11.2 kN/mm and 6.1 mm, respectively. The specimen failed at a deflection of 50 mm due to increase in the number and width of the cracks. In addition, the ductility index for this wall was 8.2, which indicated high ductility of the specimen.

3.5 W5 specimen

In this specimen, the length of the shear connectors was reduced to half (i.e. 40 mm). The purpose of this test was to investigate the effect of the shear connector length on the behavior of SC composite wall under out-of-plane loads. The deformed shape of the specimen at the end of the test is shown in Fig. 12. Due to flexural and shear cracks in the specimen, semi-ductile behavior was observed. During the loading, the first flexural crack was formed in the concrete section and by increasing the out-of-plane load, the width and depth of the cracks increased. Fig. 6(e) shows the load-displacement curve for the W5 specimen. The yield displacement and yield force of this wall was 5.9 mm and 73 kN, respectively. Failure of the specimen was first observed at a deflection of 17.2 mm with corresponding force equal to 86.6 kN. The specimen failed due to diagonal tensile cracks. The angle of these cracks was about 45 degree and failure mode of the specimen was shear failure. This failure mode happened due to short length of the shear connectors. In other words, the shear connectors (stirrups) were not able to prevent development of the diagonal cracks and these cracks extended very easily in the depth of the section.

3.6 W6 specimen

In this specimen, in addition to tensile steel plate, a compressive steel plate was utilized in order to compare the behavior of composite walls with and without compressive steel plate under out-of-plane loading. This system (steel-concrete-steel) is known as sandwich wall system. Due to difficulty in fabrication, it was not possible to weld the shear connector continuously between two steel plates. Therefore, in W6 specimen, 40 mm shear connectors were welded to each steel plate and 20 mm gap was left between the shear connectors. The deformed shape of this specimen

Fig. 14 Deformed shape of W7 specimen

is shown in Fig. 13. According to this figure, occurrence of buckling on the compressive steel plate and diagonal tensile cracks in concrete are quite clear.

Initially, few flexural cracks appeared in the W6 specimen. By increasing the load, a diagonal tensile crack started to grow in the wall section. After a while, the depth and thickness of this crack became greater than that of flexural cracks. The specimen showed yielding at a displacement of 6.6 mm and force of 87 kN, respectively. After yielding, two different phenomena occurred in this specimen at the same time. The diagonal tensile crack reached to the compressive side of the wall and the compressive steel plate buckled. Therefore, the specimen experienced two failure modes: transverse shear failure and buckling failure. As shown in Fig. 6(f), the ultimate load capacity and ultimate deflection of the specimen are 122 kN and 22.4 mm, respectively. As mentioned previously, 20 mm gap was left between the shear connectors. This gap accelerated the diagonal tensile cracks in the specimen.

3.7 W7 Specimen

In W7 specimen, the effect of concrete strength on the behavior of the SC composite walls under pure out-of-plane loads was investigated. The concrete strength of this specimen was considered 45.2 MPa. The deflected shape of this specimen was similar to that of W4 specimen. Similar to W4 specimen, this wall had a high degree of ductility and extensive cracking of concrete in the maximum moment region (Fig. 14). As shown in the load-displacement curve in Fig. 6(g), the yield strength, ultimate strength, elastic stiffness, and yield displacement of this specimen are 73 kN, 106kN, 10.8 kN/mm and 6.7 mm, respectively. The flexural cracks increased along with the depth of the section and the specimen failed at a deflection of 50 mm. At the end of the test, the upper and lower parts of the concrete rotated and separated from the surrounding elements.

3.8 W8 Specimen

In this specimen, the total number of shear connectors was reduced to six in order to evaluate the effect of large spacing between the shear connectors on the behavior of the SC composite wall under pure out-of-plane load. As observed earlier for the W2 specimen, when the spacing between the shear connectors was increased from 100 mm to 200 mm, no difference was observed in the failure mode of the specimen and it showed a high degree of ductility. In the W8 specimen, the spacing between the shear connectors was increased significantly up to 350 mm to check the effect of larger spacing between the shear connectors on the flexural behavior of the SC composite walls.

Fig. 15 shows the deformed shape of the W8 specimen at the end of the test. Initially, the flexural micro cracks appeared in the concrete and then the steel plate yielded. As shown in the load-displacement curve in Fig. 6(h), the yield strength, ultimate strength, elastic stiffness, and yield displacement were 76 kN, 87 kN, 8.9 kN/mm and 9.7 mm, respectively. After yielding, the specimen started to lose its resistance and at a deflection of 37.5 mm and a force of 77.5 kN, the specimen failed due to sudden weld fracture of the plate connection. In this specimen, due to large spacing between shear connectors (i.e., lower number of shear connectors), most of the interfacial shear between the layers was applied to weld line between the steel plate and the boundary elements. Therefore, fracture in weld connection was accelerated and subsequently the specimen failed. However, the specimen had an acceptable ductility at failure. In this specimen, despite large spacing between the shear connectors (i.e., 350 mm), no diagonal tensile cracks were observed. According to Eq. (1), the maximum distance between the shear connectors to avoid shear failure is 140 mm; however, despite 350 mm spacing between studs, no transverse shear failure was observed in this specimen. This behavior proved high efficiency of the SC composite system.

Fig. 15 Deformed shape of W8 specimen

Fig. 16 Deformed shape of W9 specimen

3.9 W9 Specimen

In this specimen, compressive reinforcement was used to examine its effect on the behavior of SC composite wall. A reinforcement network was placed on the compressive face of the specimen. This specimen was fabricated to compare with W4 specimen (without compressive reinforcement) and W6 specimen (with steel plate on compressive face). The deformed shape of the specimen is shown in Fig. 16. The yield strength, ultimate strength, elastic stiffness, and yield displacement are found as 84 kN, 109 kN, 11.2 kN/mm and 6.7 mm, respectively. This specimen had a ductile behavior up to a large deflection (46 mm), and then the strength of wall reduced and the wall failed due to growth of flexural cracks. At the end of the test, due to the crushing of the concrete, the compressive reinforcement was visible (Fig. 16).

4. Numerical investigation of composite walls under out-of-plane loads

In this section, finite element analysis was performed to simulate the specimens. A three dimensional finite element model was proposed using the finite element program ABAQUS (Hibbitt *et al*. 2011) to simulate the flexural behavior of composite walls under out-of-plane loads. ABAQUS has good capability to model and analyze nonlinear behavior of materials and to consider the interaction between different elements.

4.1 FE model

The FE model includes steel plate, concrete cover, shear connectors, and supports. The steel plate was modeled using linear quadrilateral shell element (S4R). S4R is a 4-node,

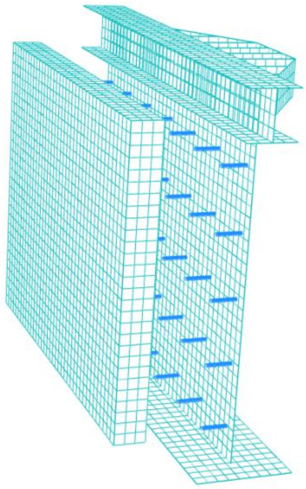

Fig. 17 The FE model of composite wall

quadrilateral, stress/displacement shell element with reduced integration and a large-strain formulation. The concrete was modeled by linear hexahedral solid element (C3D8R). The C3D8R element is a linear brick element with reduced integration. In addition, shear connectors were modeled by beam elements (B31). B31 is a 2-node linear beam with single integration point per element (Hibbitt et al 2011).

To increase the accuracy of the results, a mesh convergence study was conducted to select optimum mesh sizes. It was observed that the meshing refinement was not sensitive after having the maximum mesh size of 35 mm for shell and solid elements and 20 mm for beam elements. Fig. 17, shows the FE model of the composite wall.

The interactions and constraints definition in ABAQUS software depend on the type of the element. Furthermore, interactions and constraints should simulate the real behavior of the specimens in the lab conditions. To simulate the welded connections, a tie constraint was utilized to avoid any relative movements between the tied elements (Hibbitt *et al*. 2011). The interaction between the different layers (e.g., the interaction between steel plate and concrete cover) was defined based on surface-to-surface interaction. In the design of the specimens, it has been assumed that the shear between the layers was carried by shear connectors, therefore, the tangential behavior with zero coefficient of friction (frictionless) was considered in the interaction properties. In addition, the normal behavior (hard contact) with default properties was considered to avoid any intersect between the layers. The compressive reinforcement and shear connectors were embedded in concrete.

4.2 Material behavior, boundary conditions and loading procedure

The material properties obtained from material tests were used in the ABAQUS software. The steel plate, shear connectors and reinforcement bars were modeled as a classical elastic plastic material with Von-Mises yield criteria. The concrete damaged plasticity (CDP) model in ABAQUS was used to simulate the concrete behavior. According to the CDP model, there are two main failure mechanisms, tensile cracking and compressive crushing of the concrete. This model is applicable to different loading conditions and can be utilized for plain concrete with embedded reinforcement (Hibbitt *et al.* 2011). The material parameters to define the CDP models are dilatation angle (ψ), flow potential eccentricity ($\in$), the ratio of the biaxial compressive yield stress to the uniaxial compressive yield stress (σ_{b0}/σ_{c0}) and K_c. In this study, the amount of dilation angle (ψ), flow potential eccentricity ($\in$), stress ratio (σ_{b0}/σ_{c0}) and K_c were considered equal to 35°, 0.1, 1.16 and 0.67, respectively (Hibbitt *et al.* 2011).

The concrete compressive curve and flexural tensile strength of concrete were defined using Eq. (4) (Hognestad *et al*. 1955) and Eq. (5) (Ahmed *et al*. 2014)

$$f_c = f_c'\left[\frac{2\varepsilon_c}{\varepsilon_0} - \left(\frac{\varepsilon_c}{\varepsilon_0}\right)^2\right] \tag{4}$$

$$f_r = 0.45\left(f_c'\right)^{2/3} \tag{5}$$

where ε_c is concrete strain and ε_0 is strain when f_c reaches to f_c' and is considered equal to 0.002.

The boundary conditions were same as the test set-up. Similar to the test set-up, the load was applied very slowly with displacement control method. Due to occurrence of the excessive tensile cracks in the concrete, the Dynamic Implicit Solver was utilized instead of Static General Solver. However, to avoid any dynamic effect on the behavior of specimens and to simulate the static loading conditions, the load was applied very slowly. The force-displacement curves of the specimens were plotted to compare with the experimental results.

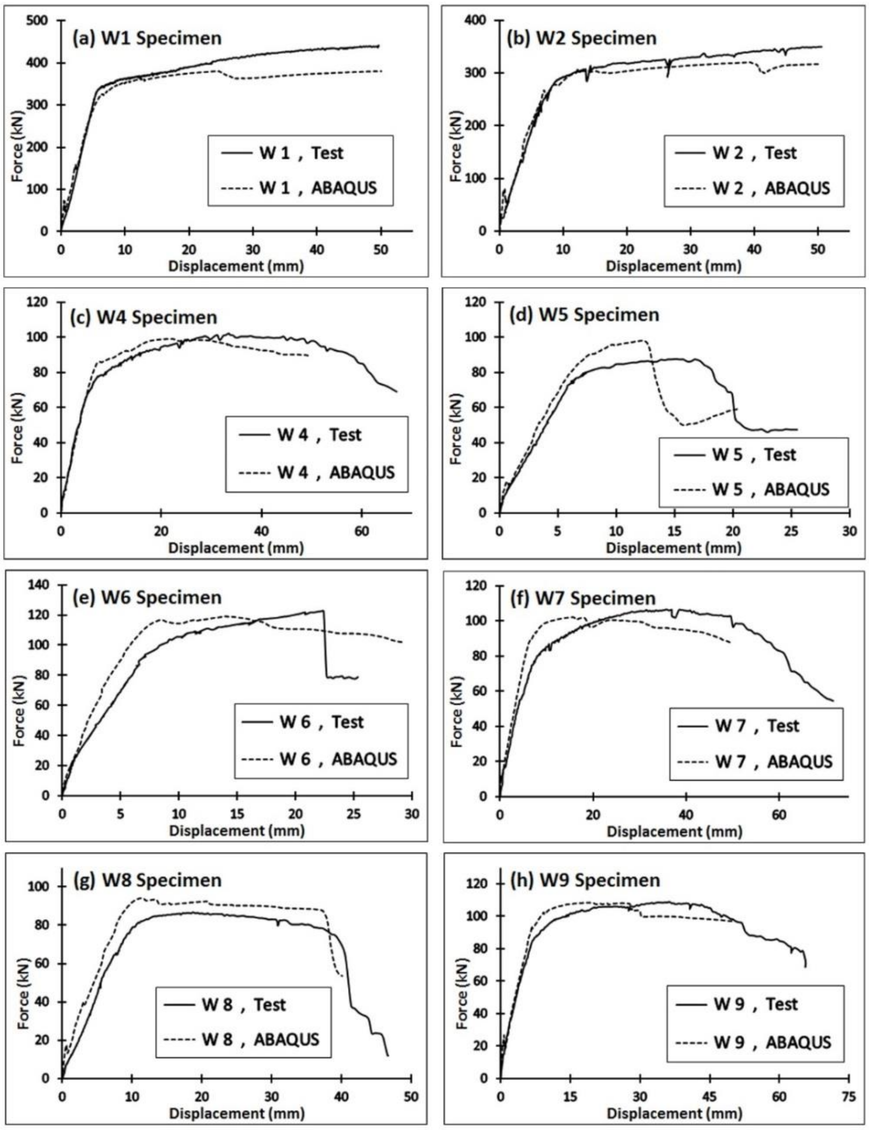

Fig. 18 Comparison of experimental and numerical load deflection curves of SC composite specimens

4.3 FE analysis results

In this section, as shown in Fig. 18, the results of finite element analyses of SC composite specimens are compared to the force-displacement curves of experimental works. As shown in Fig. 18, in all cases, the proposed FE model is reasonably accurate in predicting the behavior of SC composite walls under out-of-plane loads. The stiffness and yield strength for both experimental and numerical works were in good agreement. The small difference between the results in the nonlinear part was due to the complex behavior of concrete material. In the future studies, parametric works can be performed based on the proposed FE models. In other words, in the absence of experimental work, FE simulation would be useful to study the effect of different parameters on the behavior of SC composite walls under out-of-plane loads.

5. Flexural and shear design of SC composite walls under out-of-plane loads

In this section, the ACI 318-05 code provisions are used to calculate the out-of-plane flexural and shear strength of the proposed SC composite walls. In general, this code is developed to design the reinforced concrete beams, however, with slight modifications, it can be applied to SC composite walls. In other words, in SC composite walls, a steel plate and shear connectors are replaced with tension reinforcement and stirrups, respectively.

5.1 Flexural strength of proposed SC composite walls

According to the ACI code, following assumption are considered to derive the equations:

- The distribution of strains through the depth of section is linear.

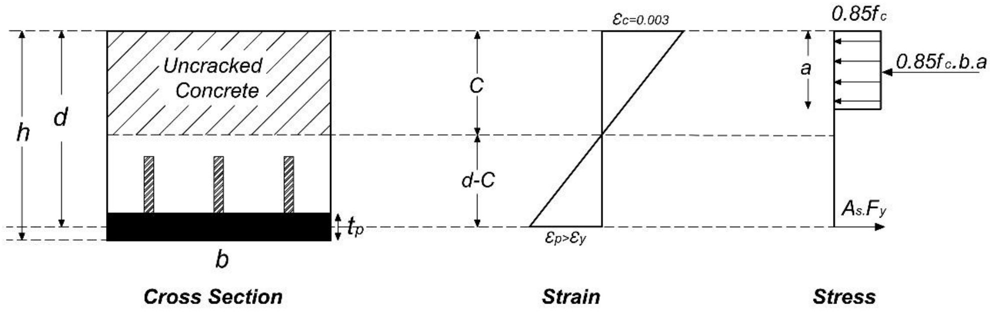

Fig. 19 Schematic view of strain and stress distribution in the height of SC composite section

- Maximum concrete compressive strain is equal to 0.003.
- Tensile strength of concrete is negligible.
- Equivalent rectangular concrete stress block is $0.85\times f_c'$.

As mentioned previously, steel plate is replaced with steel reinforcement in the tension side of section. To use the equations, it is assumed that in every section of the beam, each layer is bent to the same radius of curvature and no buckling or separation of the layers occurs. Fig. 19 shows the schematic view of strain, stress and force equilibrium in the height of the section. According to Fig. 19, using force equilibrium, the height of the stress block is derived as follow

$$a=\frac{A_s\times F_y}{0.85\times f_c'\times b} \tag{6}$$

where a is the height of the stress block, A_s is the area of steel plate, F_y is the yield stress of steel plate, f_c' is the compressive strength of concrete and b is the width of SC composite wall.

According to ACI code, the depth of the neutral axis depth is

$$C=\frac{a}{\beta} \tag{7}$$

where β is a coefficient related to concrete compressive strength and calculated as follows

$$\beta=\begin{cases}0.85 & \text{for } f_c'<30\text{ MPa}\\ 0.85\text{ - }\dfrac{0.05\times(f_c'-30)}{7} & \text{for } f_c'>30\text{ MPa}\end{cases} \tag{8}$$

Therefore, the moment capacity of the section is obtained as follows

$$M_n=A_s\times F_y\times(d-\frac{a}{2}) \tag{9}$$

Considering simply supported beam with point load at the mid span, the load capacity of the beams can be obtained with following equation

$$P=4\times\frac{M_n}{L} \tag{10}$$

In Eq. (10), the load capacity is obtained for perfect simple supports, while for the tested specimens, due to existence of welded connection and concrete cover, there was some rigidity in the supports and the rotation was not completely free in the supports. Therefore, 30 percent rigidity was considered by authors to take into account this influence of rigidity. The load capacity can be re-written as follows

$$P=1.3\times 4\times\frac{M_n}{L} \tag{11}$$

where L is the length of span.

5.2 Shear strength of proposed SC composite walls

To calculate the shear strength of the proposed SC composite wall, it is assumed that the shear connectors act as shear reinforcements (stirrups). Therefore, according to ACI code provisions, the shear strength of the section is obtained as follows

$$V_n=V_c+V_s \tag{12}$$

where V_c and V_s are the shear strength of concrete and the shear connectors, respectively.

The shear strength of concrete and the shear connectors are derived with the following equations:

$$V_c=\tfrac{1}{6}\sqrt{f_c'}\times b\times d \tag{13}$$

$$V_s=\frac{A_v\times f_{yt}\times d}{S} \tag{14}$$

where A_v is the area of the shear connectors, f_{yt} is the yield stress of the shear connectors and S is the distance between the shear connectors.

6. Results and discussion

In this section, based on the experimental program,

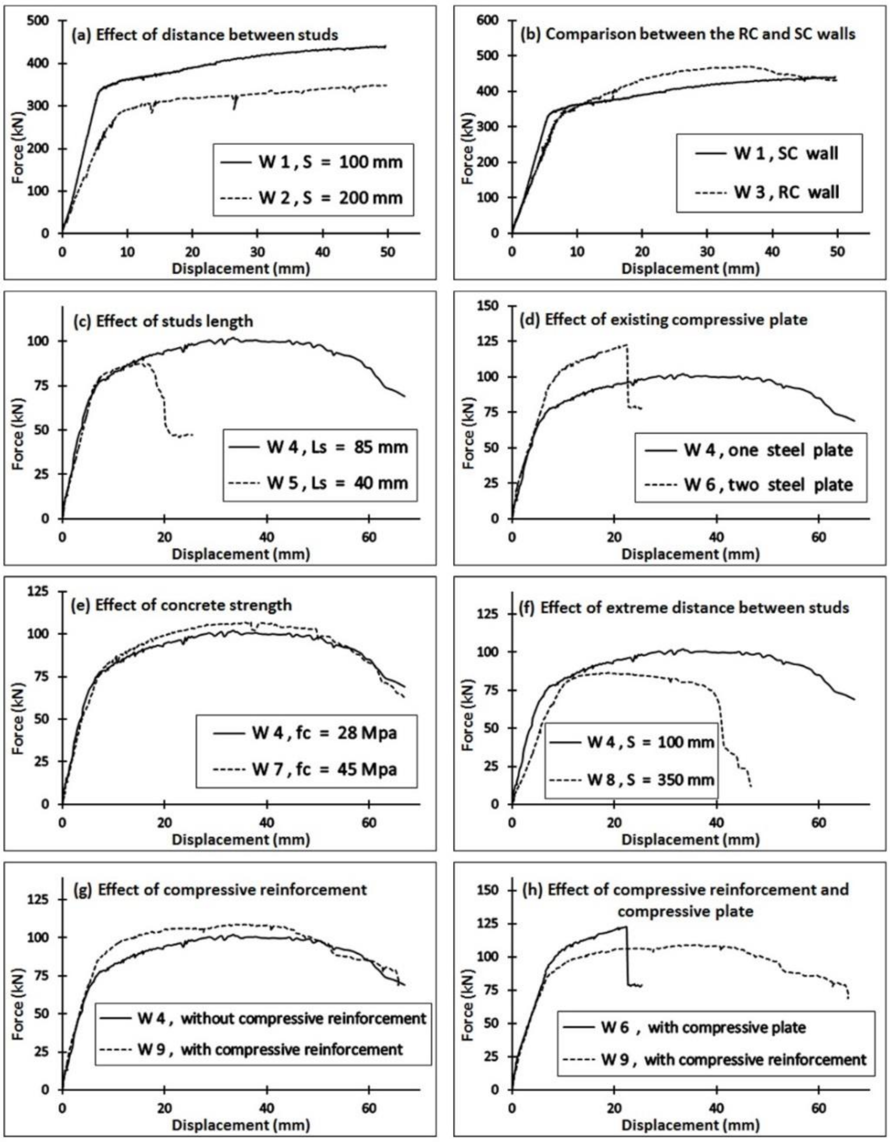

Fig. 20 Comparison between the effects of different parameters on the behavior of SC composite wall

effect of different parameters on the behavior of the SC composite walls was discussed. These parameters include spacing between the shear connectors, length of shear connectors, concrete ultimate strength, use of compressive steel reinforcement, and compressive steel plate (sandwich system). In addition, the result of the RC system was compared to the proposed SC composite wall. Furthermore, the shear strength and flexural capacity of the SC composite system were compared to design predictions according to the ACI code.

Figs. 20(a)-20(h) shows the effect of different parameters on the behavior of SC composite wall when subjected to out-of-plane loads. Details of the parametric studies are presented in the following section.

6.1 Effect of shear connector spacing on the behavior of the SC composite walls

To evaluate the effect of the shear connector spacing, W1 and W2 specimens were compared. The spacing between shear connectors in W1 and W2 were 100 mm and 200 mm, respectively. This spacing was same in both directions. By increasing the spacing, the number of the shear connectors was decreased from 130 in W1 to 35 in W2. Load-displacement curves for these two walls are shown in Fig. 20(a). According to Fig. 20(a), both specimens have ductile behavior. However, in comparison to W1, the yield strength, ultimate strength and elastic stiffness were less in W2. In SC composite structures, the shear connectors have an important role on the behavior of the specimens. By increasing the spacing (or decreasing the number) of the shear connectors, the connectivity between the layers was decreased and subsequently the stiffness and strength of the specimens reduced accordingly.

6.2 Comparison between the RC wall and SC composite walls

In this study, one RC wall (W3) was fabricated to compare with the SC composite wall (W1). Both specimens were designed based on ACI code and they had same ultimate load capacity. In W3 specimen, to provide the cover for reinforcement network, the thickness of the specimen was 40 mm more than the W1 specimen. In addition, one layer of temperature reinforcement was placed at the compressive side of the specimen. To connect the reinforcement to the upper and lower beams, a steel plate of 3 mm thickness was utilized. Fig. 20(b) shows the force-displacement curve of the W1 and W3 specimens. In the linear branch, the responses of both specimens were close to each other. In the nonlinear branch, the stiffness and ultimate load capacity of the W3 were more than W1. The possible reasons for this small difference can be due to the thickness of concrete (40 mm more than W1) and existence of reinforcement network. According to Fig. 20(b), the strength of W3 specimen dropped at a deflection of 38 mm, while in the W1 specimen, no strength reduction was observed up to deflection of 50 mm. As a conclusion, the strength of two specimens was almost same, but the ductility of the SC composite wall was better than the RC wall. However, a comprehensive study should be done to compare the efficiency of the two systems.

6.3 Effect of shear connector length on the behavior of the SC composite walls

The effect of the shear connector's length was investigated through W4 and W5 specimens. The lengths of shear connectors were 85 mm and 40 mm in W4 and W5 specimens, respectively. Fig. 20(c) shows the load-displacement curves for these two specimens. By reducing the length of shear connectors, semi-ductile behavior was observed and the specimen failed at a small deflection (17.2 mm). In other words, the W4 specimen failed in flexure with lots of flexural cracks, while the W5 specimen, due to the short length of shear connectors, failed in flexure-shear mode and diagonal tensile cracks with 45 degrees were observed. In the linear branch, the responses of both specimens were close to each other, but the ductility of the W4 specimen was much higher than W5 specimen.

6.4 Effect of compressive steel plate on the behavior of SC composite walls

In this section, the effect of presence of compressive steel plate was evaluated under out-of-plane loads. This system is known as a sandwich system and the concrete is confined between two steel plates (steel–concrete-steel). On the other hand, the proposed system only has one steel plate on the tensile side of the wall (steel–concrete). As mentioned earlier, in the sandwich system, it was not possible to weld the single and continuous shear connector between two steel plates; therefore, 40 mm length shear connectors were considered in both tensile and compressive steel plates and 20 mm gap was left between the shear connectors. This is one of the important disadvantages of the sandwich composite walls in real projects. The force-displacement curves for W4 and W6 specimens are shown in Fig. 20(d). As shown in Fig. 20(d), the ultimate capacity of the W6 is more than the W4 specimen. The difference in the ultimate strength is about 20 kN. However, the elastic stiffness of both specimens is similar. The high ultimate capacity of the W6 specimen was because of the compressive steel plate. On the other hand, the ultimate deflection of the W4 and W6 specimens were 50 mm and 22.4 mm, respectively. Therefore, the ductility of the SC composite wall (W4) was much better than the sandwich wall (W6). The brittle behavior of the W6 specimen was due to buckling in the compressive steel plate and diagonal cracks in concrete.

6.5 Effect of concrete strength on the behavior of SC composite walls

The concrete ultimate strength was another parameter that studied in this paper. Therefore, W7 specimen was built with concrete strength of 45.2 MPa and compared to the W4 specimen with concrete strength of 28.4 MPa. Fig. 20(e) shows the force-displacement curves for W7 and W4 specimens. As shown in Fig. 20(e), no considerable difference is observed. The ultimate flexural capacity of the W7 specimen increased only 4% in comparison to the W4 specimen. Thus, in the SC composite walls under out-of-plane loads, concrete strength does not has significant effect on the behavior of the specimens. This observation was in accordance with the ACI code. According to the design equations in ACI code, the concrete strength has minor effect on the flexural capacity of the specimens.

6.6 Effect of large spacing between shear connectors on the behavior of the SC composite walls

In section 5.1, the effect of spacing between shear connectors was studied and it was observed that even by doubling the distance between the shear connectors, the wall had a flexural behavior. In W8 specimen, the space between the shear connectors was increased significantly and the response was compared to the W4 specimen. In other words, the number of shear connectors was reduced from 30 in the W4 specimen to 6 in the W8 specimen. This comparison was made to evaluate the effect of the larger spacing between the shear connectors. The load-displacement curves for W4 and W8 specimens are shown in Fig. 20(f). As shown in Fig. 20(f), due to larger spacing between the shear connectors and less connectivity between the concrete and steel plate, the stiffness of the W8 specimen decreased. In addition, the W8 specimen, unlike the W4 specimen, failed at a smaller deflection of 37.5 mm.

In comparison to W4 specimen, the number of shear connectors was decreased in the W8 specimen and the shear connectors were not adequate to transfer the force to the concrete properly. This causes the force to be applied at the welded connections in the supports and the specimen failed due to weld fracture.

Table 5 Comparison of experimental results with ACI code predictions

Specimens	$P_{E\text{xp}}$ **(KN)**	$V_{E\text{xp}} = P_{E\text{xp}}/2$ **(KN)**	$P_{Eq.10}$ **(KN)**	$P_{Eq.11}$ **(KN)**	$V_{Eq.12}$ **(KN)**	$P_{E\text{xp}}/P_{Eq.10}$	$P_{E\text{xp}}/P_{Eq.11}$	$V_{E\text{xp}}/V_{Eq.12}$	**Failure mode***
W1	442	221	228.5	297	412.8	1.93	1.49	-	F
W2	350	175	228.5	297	186.8	1.53	1.18	-	F
W4	102	51	61.5	80	99.3	1.65	1.27	-	F
W5	86.6	43.3	61.5	80	27.9	1.4	1.08	1.55	F-S
W6	122	61	71.4	92.8	27.9	1.7	1.31	2.18	F-S
W7	106	53	65	84.5	106.7	1.63	1.25	-	F
W8	87	43.5	61.5	80	41.5	1.41	1.08	-	F-W
W9	109	54.5	71.4	92.8	99.3	1.52	1.17	-	F

*Failure modes: (F: flexural failure; F-S: flexural failure followed by shear failure; W: welding fracture)

6.7 Effect of compressive steel reinforcement on the behavior of SC composite walls

The W9 specimen was fabricated to study the effect of compressive steel reinforcement on the behavior of the SC composite wall. The results were compared to W4 specimen, which did not have any compressive reinforcement. In real project, compressive steel reinforcement is used as temperature reinforcement. Fig. 20(g) shows force-displacement curves for W4 and W9 specimens. As shown in Fig. 20(g), in the linear region, the results are almost same; however, the yield strength and ultimate strength of the W9 specimen are 18.3% and 6.9% higher than that of W4 specimen. In addition, the failure modes of both specimens were same.

6.8 Comparison between the effect of compressive reinforcement and compressive steel plate on behavior of SC composite wall

As mentioned in the previous sections, in the W6 specimen, a steel plate was utilized in the compressive side of the wall (sandwich system). On the other hand, compressive steel reinforcement was used in the W9 specimen. The efficiency of these methods was compared to each other. The force-displacement curves are shown in Fig. 20(h). Figure 20(h) shows that the ultimate capacity of W6 specimen is 12 % more than the W9 specimen. In addition, according to the test observations, ductile behavior was observed in the W9 specimen and the specimen failed due to flexural cracks, while brittle behavior was observed in the W6 specimen and it failed due to buckling in the compressive steel plate and diagonal tensile cracks in the concrete.

6.9 Comparison of experimental results with ACI code predictions

In this section, the results of ACI code predictions were compared with the test observations. The shear and flexural capacity of the specimens were calculated through equations presented in section 5. The results are shown in Table 5. In all of the specimens, the load capacity of the section is higher than design value. It is clear even in specimens with large distance between the shear connectors (i.e., W2 and W8), the flexural capacity of these specimens are higher than design values. In the design formulation, it is assumed that no slip takes place between layers, while in reality there is slip between the layers (depends on the number of the shear connectors and boundary elements). However, even with considering the possible slip between the layers, the experimental capacities of specimens are higher than the design code. This shows higher efficiency of the proposed SC composite system.

In W5 and W6 specimens, the flexural failure followed by shear failure (F-S) according to the test observations. Due to short length of the shear connectors, these specimens were failed in shear. Therefore, to calculate the shear resistance of these specimens, to be on the safe side, the participation of shear connectors was neglected in the formulation. The shear ratio was 1.55 and 2.18 for W5 and W6 specimens, respectively.

7. Conclusions

In this study, the idea of using SC composite walls with only one steel plate as a retaining wall system was discussed. To study the behavior of the proposed SC composite walls, an experimental program was carried out. Nine specimens were designed and tested under out-of-plane loads. In this experimental program, effect of different parameters such as spacing between shear connectors, length of shear connectors, concrete ultimate strength, compressive steel plate, and compressive steel reinforcement was investigated. Furthermore, one specimen was built with RC system to compare with the SC composite system. In addition, a 3D-FE model was proposed to study behavior of SC composite walls under out-of-plane loads. The ACI design code predictions were compared with those experimental databases to evaluate the efficiency of proposed SC composite system. The main findings of the presented work are as follows:

1. The proposed SC composite system showed very good behavior under out-of-plane loads in terms of stiffness, strength and ductility. Thus, they can be utilized as retaining walls in the deep excavation in tall buildings.
2. In the SC composite walls, due to existence of steel plate in the tension side of the specimen, the global behavior of the system was ductile enough to resist under out-of-plane loads.
3. A comparison between RC wall and SC composite wall showed that in the elastic region of the force-displacement curve, the response of both systems was almost same, but the ductility of the SC composite wall in the nonlinear region was better than the RC wall.
4. By reducing the length of the shear connectors, the failure mode of the specimen was changed from ductile to semi-ductile behavior. In other words, short length of shear connectors may cause tension diagonal cracks in the section.
5. By using compressive steel plate (sandwich system), the ultimate strength of the specimen was increased. On the other hand, due to premature buckling in the compressive steel plate and non-continuous shear connectors between the steel plates, the ductility of the specimen was decreased.
6. Increasing the concrete strength had no significant effect on the behavior of the SC composite wall (about 4 %). Therefore, instead of concrete strength, increasing the concrete cover and steel plate thickness can be effective methods to increase the capacity of the SC composite walls.
7. By using compressive steel reinforcement, the ultimate capacity of the SC composite wall was increased. However, the ductility of the specimen was not changed.
8. The use of compressive steel plate (W6 specimen) in comparison to compressive steel reinforcement (W9) increased the ultimate capacity. On the other hand, due to premature buckling in W6, the ductility of this specimen was decreased in comparison to W9 specimen.
9. In the SC composite wall, the huge part of in-plane shear force was carried by welded connection between the steel plate and boundary beams. Therefore, shear connectors would carry less shear force. This can prevent premature failure in the shear connectors and the slip between the layers can be reduced accordingly.
10. In spite of welding, connectivity between steel plate and concrete (provided by shear connectors), has a great influence on the behavior of composite system. These shear connectors increase the shear stiffness between the layers and consequently the global stiffness and strength of the section can be increased. With reduction in the number of the shear connectors, the composite system tends to behave in a separate way (no connectivity between steel plate and concrete). In W2 specimen, the number of the shear connectors was decreased from 130 to 35. This reduction leads to reduction in global stiffness and strength of the specimen.
11. According to the ACI 318, the spacing between the stirrups is limited to half of the effective depth of the section. In this study, the spacing between stirrups (e.g. distance between shear connectors in SC composite wall) in the specimens W1, W2 and W8 was two, four and seven times of the ACI 318 code allowable limitation, respectively. However, even with the larger spacing between the shear connectors, no transverse shear failure mode was observed in the specimens. This behavior shows a major advantage of using SC composite walls.
12. The proposed finite element model was able to provide good predictions for behavior of SC composite walls under out-of-plane loads. The proposed FE model can thus be used in future studies on SC composite walls.
13. The results from experimental works had higher values in comparison to ACI code predictions. In other words, the design equations in the ACI code are more conservative for SC composite walls.

References

ACI 318-05 (2005), Building code requirements for structural concrete and commentary – ACI 318R-05, American concrete institute, Farming Hills, MI, USA.

Ahmed, M., Hadi, K.M., Hasan, M.A., Mallick, J. and Ahmed, A. (2014), "Evaluating the co-relationship between concrete flexural tensile strength and compressive strength", *Int. J. Struct. Eng*., **5**(2), 115-131.

AWS (2010), Structural Welding Code—Steel. American Welding Society (AWS), D1 Committee on Structural Welding.

Cas, B., Bratina, S., Saje, M. and Planinc, I. (2004), "Non-linear analysis of composite steel-concrete beams with incomplete interaction", *Steel Compos. Struct.*, **4**(6), 489-507. https://doi.org/10.12989/scs.2004.4.6.489.

Ding, F.X., Liu, J., Liu, X.M., Guo, F.Q. and Jiang, L.Z. (2016), "Flexural stiffness of steel-concrete composite beam under positive moment", *Steel Compos. Struct.*, **20**(6), 1369-1389. http://dx.doi.org/10.12989/scs.2016.20.6.1369.

Dogan, O. and Roberts, T.M. (2010), "Comparing experimental deformations of steel-concrete-steel sandwich beams with full and partial interaction theories", *Int. J. Phys. Sci.*, **5**(10), 1544-1557.

Epackachi, S., Nguyen, N.H., Kurt, E.G., Whittaker, A.S. and Varma, A.H. (2014), "In-plane seismic behavior of rectangular steel-plate composite wall piers", *J. Struct. Eng.,* **141**(7), 04014176. https://doi.org/10.1061/(ASCE)ST.1943-541X.0001148.

Eurocode 4 (2009), Design of composite steel and concrete structures–Part 2: General rules and rules for bridges. SòTN Bratislava.

Fanaie, N., Esfahani, F.G. and Soroushnia, S. (2015), "Analytical study of composite beams with different arrangements of channel shear connectors", *Steel Compos. Struct.*, **19**(2), 485-501. http://dx.doi.org/10.12989/scs.2015.19.2.485.

Hibbitt, D., Karlsson, B. and Sorenson, P. (2011), "Simulia ABAQUS 6.11 Users' Manual".

Hognestad, E, Hanson, N.W. and McHenry, D. (1955), "Concrete stress distribution in ultimate strength design", *J. Proceedings*, **52**(12), 455-480.

Hossain, K.A. and Wright, H.D. (2004), "Experimental and theoretical behaviour of composite walling under in-plane

shear", *J Constr Steel Res.*, **60**(1), 59-83. https://doi.org/10.1016/j.jcsr.2003.08.004.
Huang, Z. and Liew, J.R. (2016), "Compressive resistance of steel-concrete-steel sandwich composite walls with J-hook connectors", *J Constr Steel Res*, **124**, 142-162. https://doi.org/10.1016/j.jcsr.2016.05.001.
Ji, X., Cheng, X., Jia, X. and Varma, A.H. (2017), "Cyclic in-plane shear behavior of double-skin composite walls in high-rise buildings", *J Struct Eng,* **143**(6), 04017025. https://doi.org/10.1061/(ASCE)ST.1943-541X.0001749.
Kurt, E.G., Varma, A.H., Booth, P. and Whittaker, A.S. (2016), "In-plane behavior and design of rectangular SC wall piers without boundary elements", *J Struct Eng*, **142**(6), 04016026. https://doi.org/10.1061/(ASCE)ST.1943-541X.0001481.
Liew, J.R. and Sohel, K.M. (2009), "Lightweight steel–concrete–steel sandwich system with J-hook connectors", *Eng. Struct.*, **31**(5), 1166-1178. https://doi.org/10.1016/j.engstruct.2009.01.013.
Oduyemi, T.O. and Wright, H.D. (1989), "An experimental investigation into the behaviour of double-skin sandwich beams", *J Constr Steel Res,* **14**(3), 197-220. https://doi.org/10.1016/0143-974X(89)90073-4.
Prabha, P., Marimuthu, V., Saravanan, M., Palani, G.S., Lakshmanan, N. and Senthil, R. (2013), "Effect of confinement on steel-concrete composite light-weight load-bearing wall panels under compression", *J Constr Steel Res.*, **81**, 11-19. https://doi.org/10.1016/j.jcsr.2012.10.008.
Qin, Y., Shu, G.P., Zhou, G.G. and Han, J.H. (2019), "Compressive behavior of double skin composite wall with different plate thicknesses", *J. Constr. Steel Res.*, **157**, 297-313. https://doi.org/10.1016/j.jcsr.2019.02.023.
Ranzi, G. (2006), "Short-and long-term analyses of composite beams with partial interaction stiffened by a longitudinal plate", *Steel Compos. Struct.*, **6**(3), 237-255. https://doi.org/10.12989/scs.2006.6.3.237.
Ranzi, G., Bradford, M.A. and Uy, B. (2003), "A general method of analysis of composite beams with partial interaction", *Steel Compos. Struct.*, **3**(3), 169-184. https://doi.org/10.12989/scs.2003.3.3.169.
Sabouri-Ghomi, S., Jahani, Y. and Bhowmick, A.K. (2016), "Partial interaction theory to analyze composite (steel–concrete) shear wall systems under pure out-of-plane loadings", *Thin Wall. Struct.*, **104**, 211-224. https://doi.org/10.1016/j.tws.2016.03.013.
Sener, K.C. and Varma, A.H. (2014), "Steel-plate composite walls: Experimental database and design for out-of-plane shear", *J. Constr. Steel Res.*, **100**, 197-210, https://doi.org/10.1016/j.jcsr.2014.04.014.
Sener, K.C., Varma, A.H. and Ayhan, D. (2015), "Steel-plate composite (SC) walls: Out-of-plane flexural behavior, database, and design", *J. Constr. Steel Res.*, **108**, 46-59. https://doi.org/10.1016/j.jcsr.2015.02.002.
Sener, K.C., Varma, A.H. and Seo, J. (2016), "Experimental and numerical investigation of the shear behavior of steel-plate composite (SC) beams without shear reinforcement", *Eng. Struct.*, **127**, 495-509, https://doi.org/10.1016/j.engstruct.2016.08.053.
Seo, J., Varma, A.H., Sener, K. and Ayhan, D. (2016), "Steel-plate composite (SC) walls: In-plane shear behavior, database, and design", *J. Constr Steel Res.*, **119**, 202-215. https://doi.org/10.1016/j.jcsr.2015.12.013.
Sohel, K.M. and Liew, J.R. (2011), "Steel–Concrete–Steel sandwich slabs with lightweight core—Static performance", *Eng Struct.,* **33**(3), 981-992. https://doi.org/10.1016/j.engstruct.2010.12.019.
Solomon, S.K., Smith, D.W. and Cusens, A.R. (1976), "Flexural tests of steel-concrete-steel sandwiches", *Mag. Concrete Res.*, **28**(94), 13-20. https://doi.org/10.1680/macr.1976.28.94.13.
Turmo, J., Lozano-Galant, J.A., Mirambell, E. and Xu, D. (2015), "Modeling composite beams with partial interaction", *J. Constr. Steel Res.,* **114**, 380-393. https://doi.org/10.1016/j.jcsr.2015.07.007.
Wright, H.D., Oduyemi, T.O. and Evans, H.R. (1991), "The design of double skin composite elements", *J. Constr. Steel Res.*, **19**(2), 111-132. https://doi.org/10.1016/0143-974X(91)90037-2.
Xie, M., Foundoukos, N. and Chapman, J.C. (2007), "Static tests on steel–concrete–steel sandwich beams", *J. Constr. Steel Res.*, **63**(6), 735-750. https://doi.org/10.1016/j.jcsr.2006.08.001
Yan, J.B., Liew, J.R. and Zhang, M.H. (2014), "Tensile resistance of J-hook connectors used in Steel-Concrete-Steel sandwich structure", *J. Constr. Steel Res.*, **100**, 146-162. https://doi.org/10.1016/j.jcsr.2014.04.023.
Yan, J.B., Liew, J.R., Zhang, M.H. and Sohel, K.M. (2015), "Experimental and analytical study on ultimate strength behavior of steel–concrete–steel sandwich composite beam structures", *Mater. Struct.*, **48**(5), 1523-1544. https://doi.org/10.1617/s11527-014-0252-4.
Yan, J.B., Wang, X.T. and Wang, T. (2018), "Compressive behaviour of normal weight concrete confined by the steel face plates in SCS sandwich wall", *Constr. Build. Mater.*, **171**, 437-454. https://doi.org/10.1016/j.conbuildmat.2018.03.143.
Yang, Y., Liu, J. and Fan, J. (2016), "Buckling behavior of double-skin composite walls: An experimental and modeling study", *J. Constr. Steel Res.*, **121**, 126-135. https://doi.org/10.1016/j.jcsr.2016.01.019.
Zhang, K., Varma, A.H., Malushte, S.R. and Gallocher, S., (2014), "Effect of shear connectors on local buckling and composite action in steel concrete composite walls", *Nucl. Eng. Des.*, **269**, 231-239. http://doi.org/10.1016/j.nucengdes.2013.08.035.
Zhao, Q. and Astaneh-Asl, A. (2004), "Cyclic behavior of traditional and innovative composite shear walls", *J. Struct. Eng.*, **130**(2), 271-284. https://doi.org/10.1061/(ASCE)0733-9445(2004)130:2(271).
Zhao, W., Guo, Q., Huang, Z., Tan, L., Chen, J. and Ye, Y. (2016), "Hysteretic model for steel–concrete composite shear walls subjected to in-plane cyclic loading", *Eng. Struct.*, **106**, 461-470. https://doi.org/10.1016/j.engstruct.2015.10.031.

DL